Functional separation of colloids and gravitoids in surface waters based on differential settling velocity: Coupled cross-flow filtration–split flow thin-cell fractionation (CFF-SPLITT)

Örjan Gustafsson[1]

Stockholm University, Institute of Applied Environmental Research (ITM), 10691 Stockholm, Sweden

Anders Düker

Stockholm University, Institute of Applied Environmental Research (ITM), 10691 Stockholm, Sweden; Swedish Museum of Natural History, Laboratory for Isotope Geology, Box 50007, 10405 Stockholm, Sweden

Jenny Larsson

Stockholm University, Institute of Applied Environmental Research (ITM) and Department of Geology and Geochemistry, 10691 Stockholm, Sweden

Per Andersson

Swedish Museum of Natural History, Laboratory for Isotope Geology, Box 50007, 10405 Stockholm, Sweden

Johan Ingri

Stockholm University, Department of Geology and Geochemistry, 10691 Stockholm, Sweden

Abstract

Given recognized challenges with shallow sediment trap and ^{234}Th-based particle flux studies, it behooves us to test the picture of surface ocean fluxes provided by such investigations with alternative and new analytical techniques. To this end, cross-flow filtration (CFF) has been coupled with split flow thin-cell fractionation (SPLITT) to afford active but mild separation of aquatic particles through a dynamic settling-velocity discrimination. Operation parameters have been developed to yield accurate settling-velocity cutoffs in the range $>0.1–>10$ m d^{-1}, element recoveries in the range 85–110%, and minimal influence of CFF preconcentration up to at least a factor 110. Chemical fingerprints of truly settling matter (i.e., gravitoids) in coastal waters provided by the CFF-SPLITT technique demonstrated that gravitoidal particles settling out of surface waters exhibit distinctly different composition than the bulk filterable particles. For instance, both gravitoidal POC and P belonged in a coastal Baltic regime largely to a slowly settling (1–2 m d^{-1}) particle pool (presumably amorphous organic aggregates), which was decoupled from a more rapidly settling (>4 m d^{-1}) Si-containing particle pool (presumably diatom dominated). Both of these biogenic gravitoid pools were in turn distinct from an Fe-containing gravitoid pool settling >4 m d^{-1}, which, in contrast to POC, P, and Si gravitoids, had a geochemical composition similar to that of bulk particles.

Importance of surface ocean export fluxes—Accurately quantifying and mechanistically understanding particle-mediated settling fluxes out of surface waters remains an important challenge in limnology and oceanography. One chief obstacle is the size overlap between colloidal (suspended) and gravitoidal (net settling) particles, complicating their functional separation and analysis (Gardner 1997; Gustafsson and Gschwend 1997; Buesseler 1998). For instance, organically coated mineral particles (small but dense) would settle much faster through the water column than many much larger but more loosely conformed organic aggregates. Hence, from a functional perspective, the small mineral-rich particles qualify as gravitoids, whereas up to millimeter-sized aggregates with near-neutral buoyancy can be said to exhibit a more colloidal behavior (Gustafsson and Gschwend 1997). Such large interparticle differences underscore that an alternative to simple size-based filtration is required in order to obtain biogeochemical fingerprints of the wide spectrum of particles with differential tendencies to settle out of surface waters. The demand for such a settling fractionation technique is stressed by the present large need to improve

---

the parameterization of the settling flux term in the current generation of large-scale biogeochemical models (Doney 1999). Relationships between different elements being processed in this important stage of the biogeochemical cycles are still calculated assuming a constant Redfield elemental ratio (Fasham 1995; Doney et al. 1996), despite several studies having demonstrated that dramatic deviations from Redfield ratios on sinking particles should be anticipated (Goldman 1988; Sambrotto et al. 1993).

Complexity of quantifying surface ocean export fluxes—Settling matter has a wide range of sources and composition and span settling velocities in the range <1 to >100 m d⁻¹ (e.g., Fowler and Knauer 1986). Much of the current picture of surface water export fluxes is based on either the vertical distribution of radionuclides or on studies of the material caught by sediment traps. Certainly the most direct method for collecting the sinking-particle export is to deploy a sediment trap, positioned below the mixed surface layer. However, both the quantity and quality of the flux estimated from shallow sediment traps have been questioned based on a number of strongly suspected artifacts, including hydrodynamic biases (Gardner 1980; Blomqvist and Kofoed 1981; Butman et al. 1986; Gust et al. 1992; Gardner 1997), problems with preservation (Knauer et al. 1984; Wakeham et al. 1993), and swimmer/surfer related issues (i.e., collection of nonsettling matter; Michaels et al. 1990; Buesseler et al. 1994, 2000).

A recent trap comparison in the Bermuda Atlantic time series (BATS) study region between the standard surface-tethered BATS trap and a neutrally buoyant sediment trap (NBST) revealed that different components of the sinking flux might be collected with different efficiencies as a function of trap design and deployment conditions (Buesseler et al. 2000). In fact, controlled studies under different horizontal flows indicate that the collection efficiency of cylindrical traps is dependent on the particle sinking speeds and thus particle types, with lower trap collection efficiencies for slower sinking particles (Baker et al. 1988; Gust et al. 1996). Gust and Kozerski (2000) concluded that trap-related winnowing can prevent collection of the full sinking-particle spectrum and constrained for the multiPIT cylinder that >95% of all particles settling at ≤5 m d⁻¹ are rejected for trap approach velocities >12 cm s⁻¹.

An increasingly applied isotope technique for studying surface water settling fluxes is the ^{234}Th deficiency proxy (summarized in Buesseler 1998). To estimate surface water settling fluxes of any particle-associated constituent X, its particulate inventory relative to that of ^{234}Th is coupled with the radioactive disequilibrium between ^{238}U and ^{234}Th in the mixed layer. The joint global ocean flux study (JGOFS) and other programs are now largely relying on the ^{234}Th method for estimating the ocean uptake of atmospheric CO_2 through balancing with the ^{234}Th-based carbon settling export (e.g., work by several groups summarized in Buesseler 1998).

The accurateness of the ^{234}Th method hinges largely on the estimated ratio of ^{234}Th to element X (for instance, particulate organic carbon, POC) being characteristic of particles carrying both elements into the subsurface depths. Approximation of this POC/^{234}Th sinking ratio has so far been limited to filters and sediment traps. However, if the traps' collection efficiencies vary with the particles' settling velocities, nonrepresentative POC/Th ratios should be anticipated. Element ratios of specific trap components deviating up to a factor of 1,000 to that of the filtered particles have been observed (e.g., Coale 1990; Buesseler et al. 1994). Similarly, the ratio of POC/^{234}Th on filtered particles has been shown to vary significantly with depth and especially with varying filter pore size (e.g., Buesseler 1998). The present inability to explicitly obtain element ratios on gravitoids has implications for the reliability of current ^{234}Th-based estimates of ocean uptake of carbon and by extension also of other elements.

SPLITT method—Two recent reviews have suggested the usage of an innovative particle sampling technique that may provide an explicit measure of the biogeochemical fingerprint on gravitoids—including element/^{234}Th ratios—as well as an independent measure of surface water settling fluxes (Gustafsson and Gschwend 1997; Lead et al. 1997). The technique termed split flow thin-cell fractionation (SPLITT) is a method where particles are separated during laminar fluid flow in a thin channel based on a combination of their hydrodynamic radius, wet density, and diffusion coefficient (Giddings 1985; Fuh et al. 1992). Hence, applied to surface water, SPLITT would have an easily adjusted cutoff that instead of being based on particle size is based on particle settling velocity. SPLITT is a gentle separation method as the resulting fractions are obtained using a virtual membrane that is a continuously renewed liquid boundary layer. The technique has so far found its widest use in biomedical applications (e.g., Levin and Tawil 1993). SPLITT has also proved quite useful in mimicking the natural hydrodynamic sorting of bottom sediments (Keil et al. 1994) and in pre-separation of river particles (Contado et al. 1997). Applied to surface ocean particles, element ratios obtained explicitly for SPLITT-fractionated gravitoids would be superior to current filtered or sediment-trapped approximations.

It is the objective of the present work to demonstrate the development and feasibility of SPLITT to contribute an improved picture of settling matter in natural waters. To this end, controlled laboratory-based method development and integrity experiments have been combined with applications to coastal surface waters to constrain the present operating range and to optimize the system configuration and running conditions.

Materials and methods

Basic principle of the SPLITT technique—SPLITT separation is based on differential lateral transport across a thin cell (Fig. 1), which resembles the channels used in the related field-flow fractionation (FFF) techniques. This construction allows for rapid, continuous separation with good resolution. The particle suspension sample is introduced through top inlet a', and a suitable carrier solution through bottom inlet b' (Fig. 1). The two flows meet and attain a laminar flow profile just beyond a thin sheet of inert material positioned at the inlet end of the cell (termed inlet splitter). The carrier flow rate $V(b')$ is generally higher than the sam-
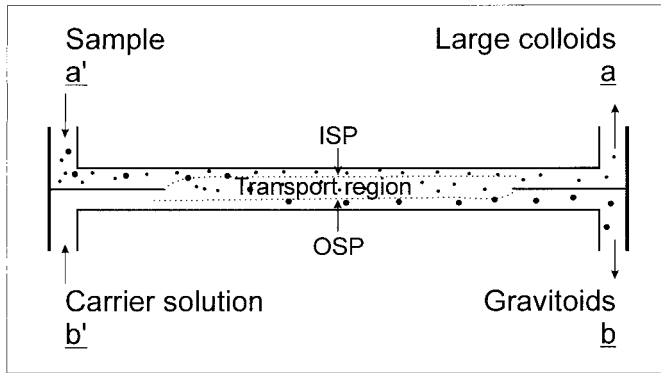
Fig. 1. The SPLITT cell (side view) consists of two glass plates separated by Teflon spacers and stainless steel splitters. The particles in the sample suspension settling from above their initial position above the inlet splitting plane (ISP) across the transport region and making it pass the virtual hydrodynamic filter represented by the outlet splitting plane (OSP) during the horizontal transport through the cell are separated as gravitoids. Cell dimensions of model SF 1000HC: breadth 4 cm, length 20 cm, height 380 μm. The sample inlet is referred to as a', the carrier inlet as b', the large colloid outlet as a, and the gravitoid outlet as b.

ple flow rate $V(a')$, thus confining the introduced particles to a thin lamina at the top of the cell, separated from the particle-free carrier solution by the inlet splitting plane (ISP, the upper broken line in Fig. 1). At the outlet end of the cell, the laminar flow is again separated in two portions by a second splitter. The ratio between the outlet flow rates, $V(a)$ and $V(b)$, defines the position of an outlet splitting plane (OSP) positioned below the ISP. The region between the two splitting planes is denoted the transport region, and a sample particle must settle across this entire region to exit the cell through outlet b as a settling-velocity defined gravitoid. The flow rate in the transport region is denoted $V(t)$ (ml min^{-1}) and is calculated from the relationship

$$V(t) = V(a) - V(a'). \quad (1)$$

The most commonly used lateral force employed in SPLITT—necessary for the fractionation—is the natural gravity field, which makes the technique suitable for studies of settling particles in the environment. SPLITT theory predicts that in order to exit through outlet b, a particle must have a settling velocity U_{settle} (cm min^{-1}) so that

$$bLU_{settle} > V(t), \quad (2)$$

where b denotes the cell breadth (cm) and L the cell length (cm) between the two splitter ends.

The cutoff settling velocity (U_{cutoff}) is arbitrarily defined as where 50% of the particles with this certain settling velocity leave the cell through each outlet. The SPLITT flow rates required to achieve a desired settling-velocity cutoff can be calculated from the relationship

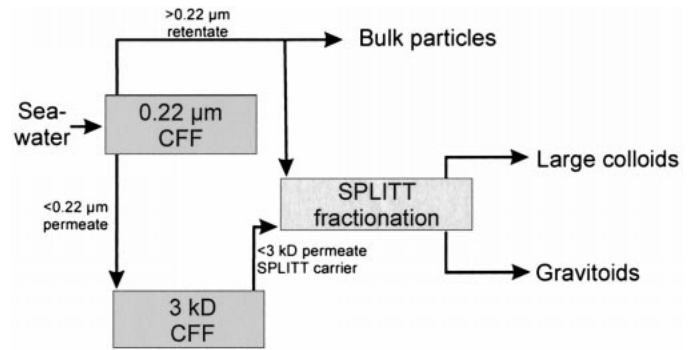$$U_{cut\text{-}off} = \frac{V(a) - \frac{1}{2}V(a')}{b \times L} \quad (3)$$

Fig. 2. Simplified flow diagram of the CFF-SPLITT system. Missing in figure are pumps, pulse dampeners/bubble traps, and online 90 + 60 μm sintered stainless steel cartridge prefilters.

The CFF-SPLITT system—For field experiments, the capacity of the SPLITT cell used in this study is generally too small to allow direct processing of the necessary water volumes in a reasonable amount of time. Hence, a particle preconcentration step was used, employing a 0.2-μm cross-flow filtration (CFF) method (Fig. 2). This CFF approach (Millipore Pellicon 2 system with 0.5 m^2 polyvinyl difluoride [PVDF] membranes) afforded generation of a more concentrated particle suspension, which facilitated analytical detection of the subsequent SPLITT fractions by reducing particles from 50 to 100 liters of natural water to about a 1-liter suspension. The <0.2-μm CFF permeate generated in this process was further ultrafiltered to remove even this portion of the colloidal particles by a 3 kD cutoff CFF (Millipore Pellicon 2; 0.5 m^2 regenerated cellulose membranes). Then, using the particle-free <3kD permeate as carrier solution, the >0.2-μm particle suspension was subjected to SPLITT fractionation to separate particles based on their differential settling velocity (Fig. 2). This sequential 0.2 μm − 3 kD CFF system is described in detail in Ingri et al. (2000). In the present study, the permeate and retentate flows were generally kept in the 200–400 and 3,000–4,000 ml min^{-1} range, respectively, yielding a crossflow ratio around 15. Exceptions were two early tests; the 0.2-μm CFF crossflow ratio during the first Landsort Deep expedition (March 1999) was around 4, and the first (May) Ekhagen Bay test was performed with ratios in the range 4–8.

The SPLITT cell employed in this study was a model SF1000HC from FFFractionation LLC. The cell consists of two glass plates separated by Teflon® spacers and stainless steel splitters. The cell dimensions were breadth 4 cm, length 20 cm, and height 380 μm. Pieces of 1.6 mm outer diameter Teflon® tubing were attached to the inlets and outlets. The sample and carrier suspensions were kept in polyethylene containers placed on a shaking table gently agitated at 40 rpm. Sample and carrier solutions were introduced to the SPLITT cell by peristaltic pumps (Cole Parmer model 7554-00, pump heads model 7013-20), using silicone tubing (Masterflex L/S 13). Both solutions were passed en route through cylinder-shaped acrylic bubble traps, which also served as pulse dampeners, placed upstream of the SPLITT inlets. Oversized particles were prevented from getting stuck in the cell by passage through two serially arranged sintered stain-

less steel cartridge-type prefilters (Swagelok SS-2F4 filter housings with SS-2F-K4 filters, 90 and 60 μm) positioned online between the pump and the pulse dampener of the SPLITT a' side. Hence, the current SPLITT system does not provide information on particles whose smallest cross-sectional diameter is larger than 60 μm.

The inlet flow rates $V(a')$ and $V(b')$ were adjusted by changing the settings on the two inlet pumps, respectively. The desired attenuation of the $V(b)$ flow rate relative to the $V(a)$ (determining the U_{cutoff}) was achieved by increasing the back pressure on the b outlet by attaching narrow-bore tubing. The SPLITT-fractionated solutions (the splittates) were collected in preweighed polyethylene flasks, and the mass of the fractions was determined by reweighing after completed collection.

Verifying SPLITT cutoffs with particle standards— SPLITT integrity experiments were performed employing well-defined spherical silica beads [7.8 μm $\pm$ 1.0 sd (error range expressed as one standard deviation [sd]), 2.52 g cm^{-3}; Duke Scientific] and similarly spherical styrene divinylbenzene particles (6.4 $\pm$ 2.0 μm sd, and 2.97 $\pm$ 0.04 μm sd, both of wet density 1.05 g cm^{-3}; Sigma Chemicals). This set of standards includes both dense inorganic particles, with settling behavior that may be representative of natural detrital particles, and low-density organic particles, which with their near-neutral buoyancy in water have a settling velocity that may be more reminiscent of loosely structured organic aggregates. The theoretical Stokesian settling velocities at 25°C of the number-based median sized particle for each type of standard are 4.4, 0.096, and 0.022 m d^{-1}, respectively. The standard beads were suspended in deionized water and processed through the SPLITT cell operated under different U_{cutoff}.

The relative masses of the standards in the two splittates were determined gravimetrically. Owing to a small but unavoidable polydispersity also of these well-defined suspensions of standard particles, their mass distribution is not proportional to the number of particles (i.e., exacerbated by the fact that large particles have larger mass). To account for this effect, the expected particle mass in the two SPLITT fractions on either side of the cutoff velocity was estimated by summation of the mass contribution from a large number of particle diameters around the mean diameter (200 steps/ standard deviation).

$$m_a = \sum_{i=0}^{d_c} p(d_i)m(d_i) \qquad m_b = \sum_{i=d_c}^{\infty} p(d_i)m(d_i) \qquad (4)$$

where m_a and m_b are the particle mass in splittate fractions a and b, d_i = particle diameter, $p(d_i)$ = probability function for this diameter, $m(d_i)$ = the corresponding particle mass for a particle of diameter d_i. The mass distribution was approximated to be normally distributed. This equation was solved numerically to yield the corrected relative fractionation of the standards into the two splittates. The model results were compared to theoretical expectations based on Stoke's Law (for number-based median sized particles), which are applicable to particles fulfilling the above ideal gravitoid standard criteria.

Application of SPLITT to natural waters—Field sites and surface water retrieval: The SPLITT system was also tested with particle suspensions obtained from one coastal location and one offshore station. Coastal samples were collected in May and June 1999 from the protected and quiescent Ekhagen Bay (59°22.54′N 18°03.58′E), just north of Stockholm on the Swedish coast of the Northwestern Baltic Sea.

Ekhagen Bay water was pumped through acid-rinsed PVC tubing from 4 m below the surface (14 m water column depth) using a rod extending from the outmost point of a pier about 50 m away from the shore. The samples were immediately transported to the Stockholm University laboratory 200 m away and CFF processing was started in a temperature-adjustable laboratory within 1 h of sampling. The bay surface water had in May a salinity of 1.2‰, T = 9°C, pH 7.2, and TOC = 7.6 mg L^{-1}, whereas the corresponding characteristics for the July 1999 Ekhagen regime were salinity of 2.9‰, T = 15°C, pH 7.2, and TOC = 4.9 mg L^{-1}.

It was also attempted to apply the CFF-SPLITT technique to the open Baltic Sea (middle of the mixed surface layer) at the time series station BY-31 (Landsort Deep; 58°36.90′N 18°14.21′E; 460 m depth, 40 km offshore of Swedish coast) in March and June of 1999. The surface mixed layer depth, POC, and TOC concentrations at these occasions were 44 m, 146 μg L^{-1}, and 5.3 mg L^{-1} (March 1999), as well as 16 m, 252 μg L^{-1}, and 4.9 mg L^{-1} (June 1999), respectively.

CFF-SPLITT fractionation of natural water suspensions: Two sets of experiments were performed with Ekhagen Bay water to investigate two key aspects of CFF-SPLITT particle separation. In the first experiment (May 1999), the SPLITT settling-velocity cutoff was kept constant at 3.0 m d^{-1} while testing the effect of varying the concentration factor of the preceding CFF preconcentration step between 47, 77, and 111. In the second series of Ekhagen Bay tests (June 1999), the CFF preconcentration factor was kept constant around 80 while varying the SPLITT flow rates to obtain the settling-velocity cutoffs: 1.0, 1.5, 2.0, 3.0, and 4.0 m d^{-1}, respectively. On the Landsort Deep expeditions, a similar set of experiments were performed.

The range of U_{settle} selected was based on estimations of average bulk settling rates from ^{238}U-^{234}Th disequilibria in Baltic Sea surface waters. In that ongoing study we are finding that the average settling velocity required of particle-associated ^{234}Th to explain the mixed layer disequilibria over an annual cycle is of the order 0.5–4 m d^{-1} (n = 18; Gustafsson et al. in prep.). As described above, there are many different combinations of flow rates that could result in a given cutoff (Eq. 3). The SPLITT flow rates used in this study to achieve the desired cutoffs are summarized in Table 1. The selected range of cutoffs also represents a good portion of the U_{cutoff} that is practicable to work with given the current SPLITT system design. In the field, we have so far operated the SF1000HC system successfully down to 0.6 m d^{-1} and up to 5 m d^{-1}. Using simple suspensions in the laboratory, we have extended this range to 0.05–10 m d^{-1}.

Subsampling and analyses of CFF-SPLITT fractions: In this method establishment study, the analytical efforts were

Table 1. Typical SPLITT flow rate settings and resulting settling velocity cutoff used (July field experiments in Ekhagen Bay).

U_{cutoff} (m d^{-1})	$V(a')$ (ml min^{-1})	$V(b')$ (ml min^{-1})	$V(a)$ (ml min^{-1})	$V(b)$ (ml min^{-1})
1.0	2.2	6.6	6.7	2.3
1.5	3.4	10.0	10.0	3.3
2.0	4.4	13.4	13.4	4.5
3.0	6.8	20.0	19.8	6.8
4.0	8.8	27.0	27.0	9.0

focused on major elements. To ensure representative sub-sampling and splitting of all sample solutions for different analyses, fractions were taken out from sample reservoirs placed on a 40 rpm shaking table by pumping peristaltically. In this way, a 20% subfraction was taken from the >0.2-μm SPLITT feed (Fig. 2). The carrier solution, as well as the large colloid and gravitoid splittates, was divided 50/50 for analyses by ICP-AES and CHN-irm-MS instruments respectively (details below). The particle suspensions for ICP analysis were collected on 47-mm diameter 0.22-μm nitrocellulose filters (Millipore), which had been prewashed in 5% acetic acid. The corresponding samples to be analyzed by CHN-irm-MS were collected on precombusted (450°C 12 h) 47 mm GF/F filters (Whatman). These vacuum filtrations—using a plastic filter holder (Nalgene) for ICP samples and a stainless steel one for CHN-irm-MS samples—were performed directly upon collection in a laminar flow clean-bench with HEPA filtered intake (Holten LaminAir A/S).

The filters were first digested in HNO$_3$ and ashed at 550°C, followed by fusion of the residue using lithium metaborate (Burman et al. 1978) prior to quantification by inductively coupled plasma/atomic emission spectroscopy (ICP-AES). Concentrations in the different particle fractions were obtained for Al, Ba, Ca, Fe, K, Mg, Mn, Na, P, Si, Sr, and Ti using ICP-AES in cooperation with SGAB Analytica AB (Luleå, Sweden). The analytical uncertainties for the ICP-AES method (expressed as ±1 sd for $n = 3$–4) is between ±10% (e.g., for Fe) and ±1% (e.g., for Si).

Quantification of particulate organic carbon (POC) was performed on dried and mildly acidified filters (following procedure in Gustafsson et al. 1997) placed in Ag capsules using a CHN elemental analyzer (Perkin Elmer CHN 2400) coupled to a Micromass Optima isotope ratio monitoring gas mass spectrometer (CHN-irm-MS).

Results and discussion

Cutoff calibration with particle standards—The results from SPLITT fractionation of particle standards largely agreed with theoretical expectations. First, it was readily possible to achieve a varying fractionation of monodisperse particles that did not simply follow the relative hydraulic flow rates (Fig. 3), confirming that a nonturbulent (laminar) flow regime indeed was established in the SPLITT cell. Theoretical estimates of the total particle mass in the two fractions were derived by integrating the masses of the particle populations expected at each side of the cutoff diameter (d_c) as described in the Methods section. Line plots of these the-
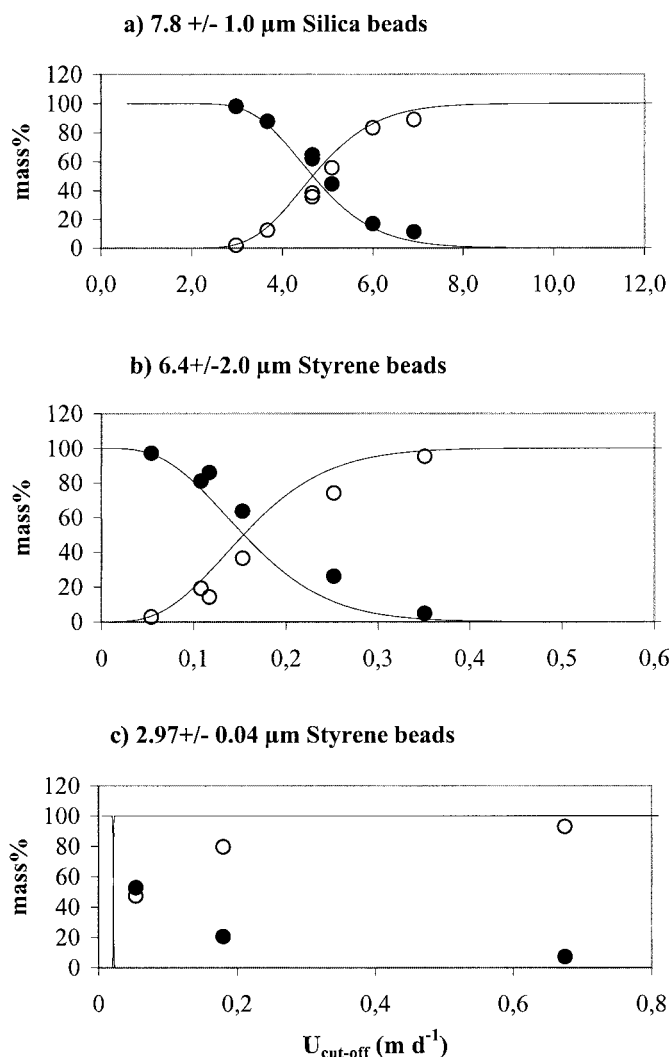

Fig. 3. Cutoff calibration graphs. The accurate separation is based on differential settling of three monodisperse spherical particle standards. The lines are theoretical fractograms predicted by Stoke's Law taking into account the non-Gaussian mass distribution (Eq. 4). Open circles are the fraction of particles operationally defined as colloids; filled circles represent the gravitoidal fraction.

oretical fractograms are overlaid on the SPLITT data in Fig. 3. The relative sharpness of the slope of these curves near U_{cutoff} reflects the degree of dispersity of the standard particle population. Overall, settling-velocity fractograms generated for the three standards were in the same range as predicted from this theoretical model and even from the simplified prediction based on Stoke's Law for the median diameter. The experimentally obtained U_{cutoff} for the 7.8-μm silica beads was 4.5–5.0 m d^{-1} (Fig. 3a). Stoke's Law for the median particle would predict 4.4 m d^{-1}, and the improved prediction from the numerical model suggested a 4.9 m d^{-1} cutoff. The settling fractogram of the 6.4-μm styrene spheres also compared quite well with theory with an obtained experimental U_{cutoff} around 0.15–0.20 m d^{-1} versus a theoretical prediction of 0.15 m d^{-1} (Fig. 3b). Finally, the particle settling distribution of the 2.97-μm styrene spheres (empirically
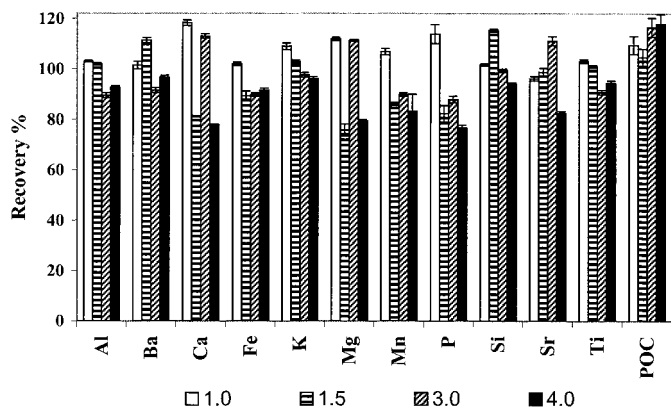
Fig. 4.   Mass recovery of major elements around the SPLITT system during fractionation of coastal Baltic Sea water in July 1999. The legend refers to different U_{settle} (m d^{-1}) cutoffs tested. Error bars represent 1 sd of the propagated analytical uncertainty derived from quadruplicate analyses.

obtained U_{cutoff} of about 0.05–0.07 m d^{-1}) compared with theoretical expectations of 0.02–0.03 m d^{-1} (Fig. 3c). The offset for this small and low-density particle may be due to its very low U_{settle} being at the lower end of the practical operating U_{cutoff} range of the present SPLITT system. Overall, these standard particle experiments demonstrate that the present SPLITT system is able to separate differentially settling particles in a dynamic, predictive, and quantitative fashion.

Elemental mass balance considerations around SPLITT— Several factors need to be considered when assessing the mass balances of the particulate inventories of elements during the SPLITT processing procedure. The recovery (*R*%) was calculated as the ratio between the amount of an element found in the sum of the large colloid and the gravitoid splittate fractions to that in the unfractionated feed fraction (i.e., bulk > 0.2 μm particles) that had been delivered into the cell:

$$R\% = \frac{n_{large\_colloids} + n_{gravitoids}}{n_{feed}} \qquad (5)$$

In the May 1999 Ekhagen experiment the *R*% of many elements was in the 70% range (data not shown). However, in the July 1999 Ekhagen experiments, the SPLITT *R*% of most elements analyzed was in the 85–110% over the range of settling-velocity cutoffs investigated (Fig. 4).

Apart from a different particle regime obviously being fractionated, we have considered a number of other potential explanations to the lower recoveries in May than in July based on aspects of the separation procedure. First, the particle concentration in the sample suspension does not seem to have an effect over the concentration ranges employed, since there was no discernable effect of CFF concentration factor (and thus particle concentration) on the observed May Ekhagen recoveries (e.g., for Fe: 73% at concentration factor [cf] 47; 71% at cf 77 and 72% at cf 111). Some losses of particulate matter in the pulse dampener were visually observed. However, ICP-AES quantification of this material

showed that it was not significant for the overall mass balance (<1% for elements analyzed). We also considered that the subsampling of the feed could have been biased if the particle suspension was not homogeneous. However, in addition to being continuously mixed on a shaking table, the subsampling tubing was not resting on the bottom of the container but was immersed only to middepth. Yet another plausible loss mechanism in SPLITT is that some rapidly sinking particles get deposited and stuck to the bottom glass plate (*see Fig. 1*). Were this process to dominate the losses, a clear trend should be discernible with larger losses in the slower settling-velocity cutoff experiments with longer cell transfer/residence times (Table 1). However, there were no apparent effects of varying settling-velocity cutoff on the observed *R*% in the July experiments (Fig. 4). It is conceivable that some particle types may be broken up into smaller filter-passing entities by the $V(a')$ pump. However, the same particle had already been passed many times through a similar peristaltic pump during the preceding CFF (with apparently reasonable recoveries; *see below*) prior to the single pump pass en route to the SPLITT cell. Further, peristaltic pumps have been demonstrated to be the mildest pump type, better preserving the particle integrity than other designs (Gibbs 1981). Shorter hold-up times between CFF and SPLITT stages and longer postprocessing flushing times and cell cleaning could be two reasons contributing to yield the high and acceptable recoveries of the more recent experiments. The July 1999 Ekhagen experiments demonstrate that good recovery of different elements is obtainable with the present SPLITT system (Fig. 4). No effect on elemental mass balance from CFF concentration factor or of SPLITT settling-velocity cutoff was observed.

Effects of varying CFF conditions—The overall reliability of CFF-SPLITT results will obviously depend also on the CFF step. The 0.2-μm CFF system relied upon in this study was used in a previous study of colloid dynamics in the Kalix River estuary, where photon correlation spectroscopy of the permeate suggested that no particles larger than 0.1– 0.2 μm indeed did pass through the PVDF membrane (Gustafsson et al. 2000). In other studies aimed specifically at investigating the integrity of various CFF systems, we have found that a high retentate/permeate (i.e., cross flow, CF) ratio yields smaller losses to the CFF membrane (Gustafsson et al. 1996; Larsson et al. in prep.). Field recovery of POC around the 0.2-μm CFF membrane can be used to test the recovery of this system. Different CF ratios were shown to have a large effect on the ability to concentrate POC from surface waters without artifacts. Open Baltic Sea surface water POC at time series station BY-31 (Landsort Deep) in March 1999 calculated from 47 mm GF/F sampling of the 0.2-μm CFF retentate in six consecutive runs was in the range 3–30 μg L^{-1}. This is significantly less than the 160 μg L^{-1} obtained simultaneously on similar GF/F filters but employing 293 mm diameter GF/F filters and high-volume filtration techniques (Gustafsson et al. in prep.). The low CF ratios—in the range 3–8—employed at that occasion probably account for the poor CFF recoveries of POC. Hence, with such dubious results from the CFF preconcentration stage, any subsequent SPLITT results could not be trusted

Table 2. The POC concentration determined on GF/F filters in the >0.2 μm CFF retentate, and in the CFF-SPLITT gravitoid fractions (both corrected for the CFF concentration factor, and the SPLITT dilution factor, respectively), as well as POC from regular direct filtration for comparison.

Regime	U_{settle} (m d^{-1})	CFF cf (−)	POC* (μg L^{-1})	CFF POC (μg L^{-1})	Gravitoidal POC (μg L^{-1})
BY-31:					
14 June 1999	3.0	24	130–390	135	2.0
14 June 1999	3.0	49	130–390	75	2.2
15 June 1999	3.0	99	130–390	107	2.6
16 June 1999	3.0	233	130–390	119	0.9
17 June 1999	1.5	102	130–390	189	6.5
17 June 1999	1.5	151	130–390	80	2.7
16 June 1999	1.5	180	130–390	197	11.7
EKH:					
7 July 1999	4.0	109	200–700	350	4.0
6 July 1999	3.0	84	200–700	513	4.2
8 July 1999	2.0	74	200–700	292	25.3
6 July 1999	1.5	83	200–700	390	20.4
7 July 1999	1.0	102	200–700	384	40.6

* POC from the same regime (BY-31; Broman et al. 1991; Gustafsson et al. in prep.; Walve and Larsson 1999) or similar coastal Northern Baltic regimes (EKH July; coastal Northern Baltic: Andersson and Rudehäll 1993; Heiskanen and Läppanen 1995).

as a reliable representation of in situ settling behavior. In contrast, on a subsequent BY-31 field campaign in June 1999 with CF ratios >10, the POC concentrations calculated from seven 0.2-μm retentates collected during the course of a week and spanning concentration factors 24–233 were consistently in the range 80–200 μg L^{-1} (Table 2). Given the well-known variability of a factor of 2–3 between high-volume and low-volume POCs (e.g., Buesseler 1998; Moran et al. 1999), this is interpreted as not significantly different from the high-volume POC of 252 μg L^{-1} obtained at that expedition. Other investigations at this offshore station are reporting POC concentrations in the range 130–390 μg L^{-1}

at this time of year (refs. in Table 2). In the July Ekhagen Bay experiments presented below, the CF ratios were kept around 15. Unfortunately, no separate non-CFF concentrated POC sample was taken at that occasion. However, the concentration-factor corrected CFF retentate samples suggested an Ekhagen Bay POC concentration in the range 300–500 μg L^{-1} (Table 2; no trends with CFF preconcentration factor), which is what might be expected for a coastal north-central Baltic regime at this time of year (refs. in Table 2). The difficulty of sampling large fragile aggregates is recognized. The present CFF recovery data for POC suggest that breakup of large aggregates is not a significant process during the comparatively mild cross-flow filtration and thus does not appear to be affecting the CFF-SPLITT results. This is further supported by the fact that the CFF-SPLITT-derived vertical POC flux is not significantly smaller than the flux obtained by other methods (Table 3).

The effect of varying CFF concentration factor (cf) on CFF-SPLITT results was investigated in the May 1999 Ekhagen Bay experiment. The geochemical signal in the three particulate SPLITT pools; feed (CFF retentate), large colloid splittate, and gravitoid splittate, did not appear to follow a cf trend (Fig. 5). In order to investigate whether the composition in each of the three pools varied as a function of cf, the particulate inventory of the major elements Fe, POC, and Si were normalized to that of Al (mass basis). Using such source- and process-diagnostic element ratios also removes potential systematic errors in the handling and analyses. Overall there were only small variations in any of the element ratios in the different pools as a function of cf. The Fe/Al ratio was around 0.5 at all three cf's and in all the three particulate pools (Fig. 5a). The gravitoidal Si/Al (Fig. 5b) and POC/Al (Fig. 5c) ratios were higher than in the feed and large colloidal pool at all three cf's. However, whereas a minor decreasing trend with increasing cf might be seen in the gravitoid Si/Al ratio, no trend was observable for the corresponding POC/Al ratio. In addition to some losses during SPLITT fractionation in this May experiment, it should

Table 3. The POC flux at station BY-31 in different settling velocity bins from CFF-SPLITT compared with bulk flux estimates from sediment trap and ^{234}Th proxy methods during the same period. The sediment trap and ^{234}Th-based POC fluxes is from a parallel but separate study (BY-31; Gustafsson et al. in prep).

Regime	U_{settle} range (m d^{-1})	CFF-SPLITT (mmol m^{-2} d^{-1})	Sediment trap (mmol m^{-2} d^{-1})	^{234}Th-POC$_{filter}$* (mmol m^{-2} d^{-1})	^{234}Th-POC$_{trap}$† (mmol m^{-2} d^{-1})
BY-31					
June 1999	1.5–3.0	1.0			
June 1999	>3.0 (avg. 3)‡	0.5			
June 1999	>3.0 (avg. 10)‡	1.6			
May–Aug 1999	bulk		2–9		
May–Aug 1999	bulk proxy			42–94	3–8
EKH					
July 1999	1.0–2.0	3.2			
July 1999	2.0–4.0	4.4			
July 1999	1.0–4.0	7.6			
July 1999	>4.0 (avg. 4)‡	1.3			
July 1999	>4.0 (avg. 10)‡	3.4			

* Approximating the settling POC/^{234}Th ratio from GF/F filters ($n = 3$).

† Approximating the settling POC/^{234}Th ratio from sediment trapped material ($n = 3$).

‡ Assuming different average (avg.) settling velocity of particles in the gravitoid fraction in calculating the vertical flux.
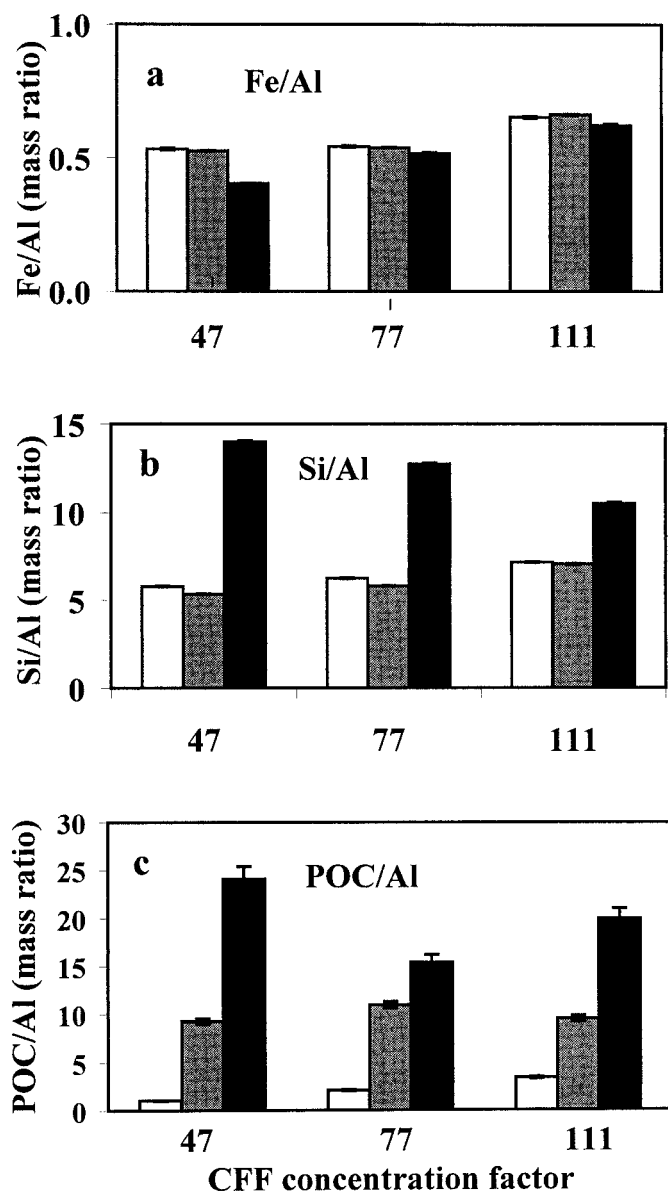
Fig. 5.   Effect of varying CFF preconcentration factors on the obtained SPLITT fractions (elemental mass ratios) in coastal Baltic water May 1999. A 3.0 m d^{-1} U_{settle} cutoff was used throughout. The leftmost open bars are the retentate/feed; the middle gray bars represent the colloidal splittate; the rightmost dark bars are the gravitoid splittate. Error bars represent 1 sd of the propagated analytical uncertainty derived from quadruplicate analyses.

also be recognized that some of the observed variability may be due to the natural particle/phytoplankton succession of the sampled regime since the water for the different cf runs was sampled on two separate days. We conclude that increasing the cf factor in the range 47–111 does not give rise to an observable effect on the geochemical signature in the subsequently isolated SPLITT fractions.

A further test of the effect of changing concentration factor on the resultant CFF-SPLITT gravitoid fractionation was conducted at the offshore station BY-31 in June 1999. Using a constant U_{settle} cutoff of 3.0 m d^{-1}, the preceding CFF was

performed in four serial experiments with the cf varied to span the range 24–233 (Table 2). Correcting the POC values obtained in the gravitoid splittate for CFF concentration factor and for SPLITT dilution factor allowed estimation of gravitoid POC (G-POC). A good repeatability was found over the several days long exercise with G-POC of 1.9 $\pm$ 0.8 μg L^{-1} (± 1 sd, $n = 4$). A similar experiment with U_{cutoff} of 1.5 m d^{-1} and CFF cf of 102–180 gave a higher G-POC of 7 $\pm$ 4 μg L^{-1} (± 1 sd, $n = 3$), consistent with its inclusion of some slower settling particles (Table 2). Hence, good integrity of the CFF preconcentration step was concluded based on high CFF recoveries and preservation of the biogeochemical signature into the CFF-SPLITT gravitoid isolate over a wide range of particle concentrations.

Biogeochemical signatures across settling-velocity spectra—The functional distribution of particulate iron and silica: Having demonstrated that important operational criteria of the CFF-SPLITT system can be met, the technique was applied to elucidate whether differential biogeochemical signals exist as a function of particle settling velocity. Settling-velocity spectra for major elements in Ekhagen Bay surface waters were determined using CFF-SPLITT in July 1999 (Fig. 6). Although these spectra (with constant CFF cf and varying the SPLITT U_{cutoff}) were developed through five different CFF-SPLITT experiments performed over the course of three days, the constant element ratios in the CFF retentate (bulk particles; SPLITT feed) indicate that the system was in a relative steady state affording comparison between the successive settling-velocity experiments. The Fe/Al ratio in the feed suspension was close to the average crust value (0.5 on a mass basis; Krauskopf and Bird 1995), and this ratio was preserved into both the large colloid and gravitoid splittates (Fig. 6a). One interpretation is that all the particulate Fe was predominantly existing in detrital particles. However, due to their high densities, such mineral particles would be expected to settle to a much larger extent than what was observed for Fe (e.g., Stoke's Law for $\rho = 2.5$ g cm^{-3} would for a 10-μm radius particle predict a settling rate of 30 m d^{-1}). However, only 1–2% of particulate Fe settled faster than 1 m d^{-1} (Fig. 7). Given that Fe in Baltic rivers is dominated by nondetrital amorphous forms (e.g., Pontér et al. 1990; Ingri and Widerlund 1994; Gustafsson et al. 2000), a significant fraction of the suspended Fe in the Baltic system (e.g., Ingri et al. 1990; Andersson et al. 1994) may result from a combination of intimately linked iron oxyhydroxides and Fe-Al-humic aggregates (cf. with the rare earth element carrier phases in rivers as discussed by Ingri et al. 2000). Nevertheless, it cannot be excluded that detrital Fe-Al particles are held in suspension by a relatively large organic coating.

In contrast, the Si/Al ratio in the feed suspension was not transferred into both splittates (Fig. 6b). Although the Si/Al ratio in the large colloidal particles was similar to the unfractionated particle pool, the CFF-SPLITT results revealed a clearly elevated Si/Al ratio in the gravitoidal pool. The Si/Al ratio for the different classes of gravitoids was constant in the >1–>4 m d^{-1} range and nearly twice as high as in the feed. The constancy of this ratio across the settling-velocity spectrum suggests that the settling particles bringing
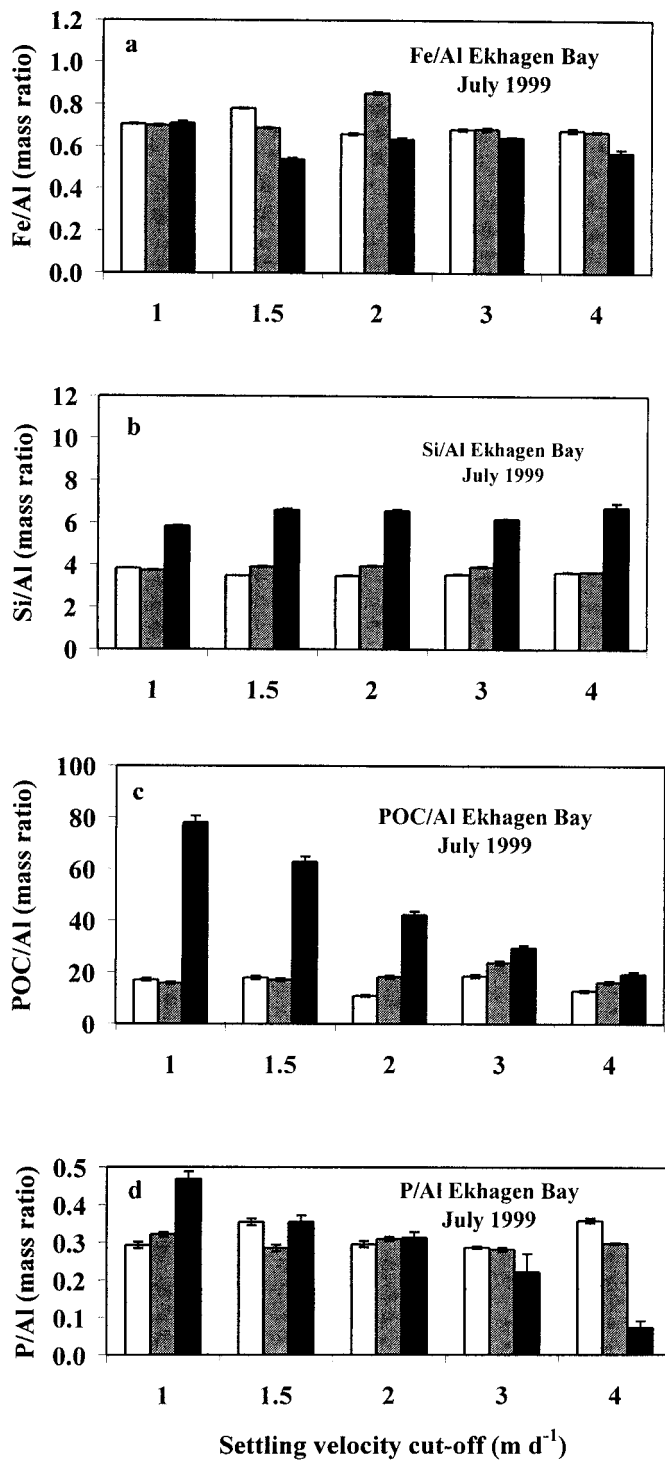
Fig. 6. Biogeochemical composition of bulk, colloidal, and gravitoidal particles defined over a range of U_{settle} in coastal Baltic surface water July 1999. A CFF preconcentration factor near 80 was used throughout. The leftmost open bars are the retentate/feed; the middle gray bars represent the colloidal splittate; the rightmost dark bars are the gravitoid splittate. Error bars represent 1 sd of the propagated analytical uncertainty derived from quadruplicate analyses.
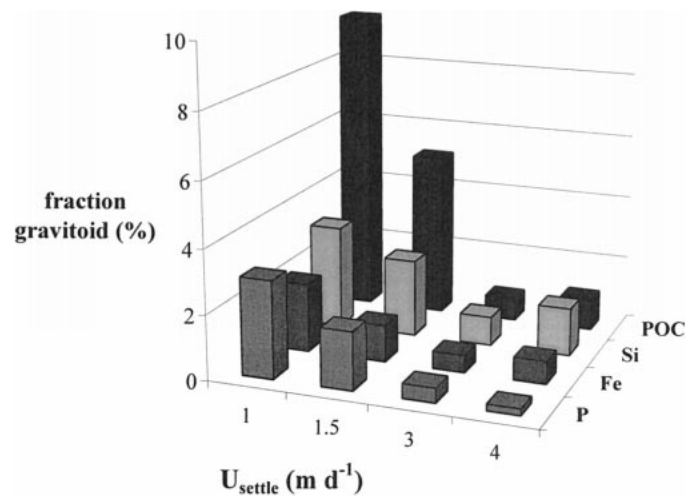

Fig. 7. Fractions of particulate elements in the gravitoidal form as defined by a range of U_{settle} cutoffs in coastal Baltic Sea water July 1999.

down Si are predominantly settling at speeds greater than the fastest cutoff in this study (i.e., >4 m d^{-1}). This is consistent with coastal diatoms accounting for the rapidly settling Si-containing particles in the July experiments. Earlier in the season during the CFF concentration-factor test (May 1999), the Si/Al ratio in the >3 m d^{-1} gravitoids was even further elevated and in the range 11–14 (Fig. 5). At that time, diatoms presumably made a significant contribution to the overall Si content of the bulk particles in these coastal surface waters since the Si/Al ratio in the feed suspension was around 6, whereas this ratio had decreased to around 4 in July. These results are consistent with a spring diatom bloom more significantly affecting the overall particle dynamics in May than in July in coastal Baltic waters (e.g., Hobro 1979; Andersson et al. 1996). Rapid settling of coastal diatoms following spring blooms has been well documented elsewhere (e.g., Waite et al. 1992; Kepkay et al. 1997). The unique information added by CFF-SPLITT data aids in elucidating the extent to which biogeochemical signatures distribute themselves across a spectrum of quantitatively defined suspended versus settling particles.

The functional distribution of particulate organic carbon and phosphorus: A clear colloid-gravitoid fractionation in the distribution of other bioactive elements also became apparent from the CFF-SPLITT results. The POC/Al ratio in all gravitoid isolates was significantly elevated compared to the ratio in bulk surface water particles (Fig. 6c). Further, this ratio increased continuously with decreasing settling-velocity cutoff from a value around 20 for the >4.0 m d^{-1} gravitoids to near 80 for the slowly settling >1.0 m d^{-1} gravitoids. Although a portion of the >4.0 m d^{-1} settling organic carbon may be associated with rapidly sinking coastal diatoms, the gravitoid spectra revealed that there exists a clear decoupling between the Si and POC settling pools in this coastal regime. The bulk of the sedimenting organic matter appears to settle much slower than Si. This may be interpreted as evidence that loosely structured amorphous

and organic-rich aggregates with low wet densities (e.g., Alldredge and Silver 1988) under some conditions are playing a quantitatively more important role than rapidly settling diatoms in the vertical export of POC from surface waters.

There was no significant trend in the P/Al in the suspended large colloids in the range <1–<4 m d^{-1}. Similar to the situation for POC, the P/Al ratio on gravitoids was distinctly different from the bulk unfractionated particle pool and was increasing with smaller settling-velocity cutoffs (Fig. 6d). However, in contrast to the POC/Al gravitoid values, the P/Al values were lower than the bulk particle signal for gravitoids >4 m d^{-1}, but steadily increasing with lower U_{cutoff} to become similar to the bulk particle signal at >2 m d^{-1} and significantly larger at >1 m d^{-1} (Fig. 6d). It is plausible that the lower P/Al in faster sinking gravitoids (>4 m d^{-1}) relative to bulk particles and slower settling gravitoids (1–4 m d^{-1}) results from (a) high P/Al in suspended and/or slowly settling living cells and freshly produced phytoplankton exudates, and (b) lower P/Al in (dead?) diatoms than in other phytoplankton (on splittates collected a few months later, SEM images revealed the presence of bare diatom frustules in gravitoid fractions, but not in large colloid fraction; data/image not shown).

Clearly, both gravitoidal POC and P belong largely to biogenic and slowly settling (≤ 1–2 m d^{-1}) particle pools in this regime, both of which appear decoupled from a similarly biogenic but more rapidly settling (>4 m d^{-1}) Si-containing particle pool. In turn, these biogenic gravitoid pools are distinct from the Fe-containing gravitoid pool settling >4 m d^{-1}.

Fraction of elements in different settling-velocity ranges—The apportionment of an element to different settling-velocity bins is useful for comprehending the particle dynamics. Only a minor portion of the standing stock of bulk particles in the Ekhagen Bay (July 1999) surface water was settling >1 m d^{-1}. For elements such as Fe, POC, P, and Si, less than 2% of the >0.2-μm particles was settling at speeds faster than 4 m d^{-1} (Fig. 7). And even for a slow settling-velocity cutoff, such as 1 m d^{-1}, it was found that only 2–3% of Fe, P, and Si and 8–10% of POC were settling. Although the settling-velocity spectra were different and characteristic to each element, as discussed above, it was observed that there was a generally increasing fraction of gravitoids with decreasing U_{settle} cutoff. The absence of an opposite trend supports that the SPLITT technique is providing physically consistent results.

SPLITT also offers the possibility to independently estimate a vertical flux. For example, at the open Baltic Sea station BY-31 in June 1999, the vertical POC flux in the 1.5–3 m d^{-1} interval was about 1 mmol m^{-2} d^{-1} (Table 3), which appears to be a significant portion of the bulk flux over the entire settling spectrum at this time. This settling-velocity-bin fractionated estimate of vertical POC flux may be contrasted to estimates of the unfractionated, or bulk, POC flux from traditional methods such as sediment traps and the ^{234}Th proxy. The POC flux—in discrete settling flux bins—obtained from this initial CFF-SPLITT study is at the lower end of what might be obtained with cylindrical sediment traps of aspect ratio 5 and the ^{234}Th proxy, when approximating the POC/^{234}Th ratio on gravitoids from the sediment-trapped material (Table 3). A much larger number for the POC flux would be estimated if the gravitoidal POC/^{234}Th ratio is approximated in the common fashion from the ratio on GF/F filters (nominally 0.7 μm). Interpretation of a time series study of trap and ^{234}Th-generated POC fluxes will be presented elsewhere (Gustafsson et al. in prep.). The G-POC data generated over a range of U_{settle} cutoffs (Table 2) facilitated a picture of the settling-velocity fractionated POC flux behavior also at the coastal Ekhagen station (Table 3). This data quantitatively underlines the importance of slowly settling particles for the total POC flux, constrained from the evolution of the compositional data over a range of settling velocities seen above (Fig. 6c). The vertical POC flux in the 1–4 m d^{-1} interval was 7.6 mmol m^{-2} d^{-1}, using the gravitoidal POC from the >1 m d^{-1} splittate and an average U_{settle} of 2.5 m d^{-1}. The >4 m d^{-1} gravitoid data suggested a vertical POC flux for this settling component of 1.3 mmol m^{-2} d^{-1}, assuming a U_{settle} of 4 m d^{-1} (3.4 mmol m^{-2} d^{-1} if the average U_{settle} for gravitoids settling >4 m d^{-1} is 10 m d^{-1}). The settling-velocity fractionated picture of, for instance, the POC flux is unique information made possible with the SPLITT technique, which complements the bulk integrated POC flux obtainable from either the ^{234}Th method or sediment traps.

The SPLITT vision on ocean flux studies: potential implications—Given recognized challenges with sediment trap and ^{234}Th-based particle flux studies, it behooves us to consider whether our present understanding of surface ocean fluxes is to any extent skewed by biases inherent in either of these two methods. The new perspective on settling particles afforded by the CFF-SPLITT technique may be one of several rewarding ways to afford such testing. This technique can provide chemical fingerprints of truly settling matter. Such information is in high demand for many marine research questions, including parameterizing large-scale biogeochemical models and an increased understanding of the biogeochemical cycles (e.g., Doney 1999). Recently, the role of heavy minerogenic sinkers—presumably making up only a small portion of bulk aggregate volume—on particulate matter settling has been discussed (e.g., Hernes et al. pers. comm.; Gustafsson et al. 2000). This and other hypotheses on trigger mechanisms of vertical fluxes may be favorably tested with the CFF-SPLITT method. Finally, the POC/^{234}Th ratio now obtainable on truly settling particles (i.e., gravitoids) from direct sampling of the mixed surface ocean is likely to improve the current ^{234}Th-based ocean POC sinking flux estimates. Currently, most of those studies are assuming that POC/^{234}Th ratios obtained with size-based filtration are identical to the signal on gravitoids.

Ultimately, improved sediment-trap technology (e.g., neutrally buoyant traps; Buesseler et al. 2000) and SPLITT fractionation techniques may prove complementary. It appears that sediment traps are better at sampling rapidly sinking particles but may miss a dominant fraction of the slowly settling matter (e.g., Baker et al. 1988; Gust et al. 1996, Buesseler et al. 2000; Gust and Kozerski 2000). In contrast, The SPLITT cell employed in this study is well suited to shed light on particles settling as slowly as 1 m d^{-1}. Infor-

mation from the SPLITT technique is limited in time reso-
lution to approximately 1 h–1 d. Individual trap collections
and [234]Th proxy data operate over the days–months time
scale. Further, whereas a sediment trap provides a settling-
velocity integrated sample of the bulk settling matter, frac-
tions from the SPLITT method provide a dynamic picture
of the biogeochemical composition across user-defined set-
tling-velocity spectra.

Further developments in application of SPLITT technol-
ogy to study ocean particle dynamics could favorably in-
clude employing a separation cell with higher capacity. An
extra-high capacity (EHC) SPLITT cell is available that
would enable processing of 18 times more sample in a given
amount of time. Preconcentration of particles prior to
SPLITT fractionation may not be required for some mea-
surements with the EHC cell. Instead, the CFF could be
applied in a postconcentration mode to the separated split-
tates (i.e., SPLITT-CFF).

References

ALLDREDGE, A. L., AND M. W. SILVER. 1988. Characteristics, dy-
namics and significance of marine snow. Prog. Oceanogr. **20:**
41–82.

ANDERSSON, A., S. HAJDU, P. HAECKY, J. KUPARINEN, AND J. WIK-
NER. 1996. Succession and growth limitation of phytoplankton
in the Gulf of Bothnia (Baltic Sea). Mar. Biol. **126:** 791–801.

———, AND Å. RUDEHÄLL. 1993. Proportion of plankton biomass
in particulate organic carbon in the Northern Baltic Sea. Mar.
Ecol. Prog. Ser. **95:** 133–139.

ANDERSSON, P. S., G. J. WASSERBURG, J. INGRI, AND M. C. STOR-
DAL. 1994. Strontium, dissolved and particulate loads in fresh
and brackish waters: The Baltic Sea and the Mississippi Delta.
Earth Planet. Sci. Lett. **124:** 195–210.

BAKER, E. T., H. B. MILBURN, AND D. A. TENNANT. 1988. Field
assessment of sediment trap efficiency under varying flow con-
ditions. J. Mar. Res. **46:** 573–592.

BLOMQVIST, S., AND C. KOFOED. 1981. Sediment trapping—a sub-
aquatic in situ experiment. Limnol. Oceanogr. **26:** 585–590.

BROMAN, D. C., C. R. NÄF, AND Y. ZEBUHR. 1991. Occurrence and
dynamics of polychlorinated dibenzo-p-dioxins and dibenzo-
furans and polycyclic aromatic hydrocarbons in the mixed sur-
face layer of remote coastal and offshore waters of the Baltic.
Environ. Sci. Technol. **25:** 1850–1864.

BUESSELER, K. O. 1998. The decoupling of production and partic-
ulate export in the surface ocean. Glob. Biogeochem. Cycles
12: 297–310.

———, A. F. MICHAELS, D. A. SIEGEL, AND A. H. KNAP. 1994. A
three-dimensional time-dependent approach to calibrating sed-
iment trap fluxes. Glob. Biogeochem. Cycles **8:** 179–193.

———, D. K. STEINBERG, A. F. MICHAELS, R. J. JOHNSON, J. E.
ANDREWS, J. R. VALDES, AND J. F. PRICE. 2000. A comparison
of the quantity and composition of material caught in a neu-
trally buoyant versus surface-tethered sediment trap. Deep-Sea
Res. I. **47:** 277–294.

BURMAN, J.-O., C. PONTÉR, AND K. BOSTRÖM. 1978. Metaborate
digestion procedure for inductively coupled plasma-optical
emission spectrometry. Anal. Chem. **50:** 679–680.

BUTMAN, C. A., W. D. GRANT, AND K. D. STOLZENBACH. 1986.
Predictions of sediment trap biases in turbulent flows: A the-
oretical analysis based on observations from the literature. J.
Mar. Res. **44:** 601–644.

COALE, K. H. 1990. Labyrinth of doom: A device to minimize the
"swimmer" component in sediment trap collections. Limnol.
Oceanogr. **35:** 1376–1381.

CONTADO, C., F. DONDI, R. BECKETT, AND J. C. GIDDINGS. 1997.
Separation of particulate samples by SPLITT fractionation us-
ing different operating modes. Anal. Chim. Acta **345:** 99–110.

DONEY, S. C. 1999. Major challenges confronting marine biogeo-
chemical modeling. Glob. Biogeocem. Cycles **13:** 705–714.

———, D. M. GLOVER, AND R. G. NAJJAR. 1996. A new coupled,
one-dimensional biological-physical model for the upper
ocean: Applications to the JGOFS Bermuda Atlantic Time Se-
ries Study (BATS) site. Deep-Sea Res. II **43:** 591–624.

FASHAM, M. J. R. 1995. Variations in the seasonal cycle of biolog-
ical production in subarctic oceans: A model sensitivity anal-
ysis. Deep-Sea Res. I **42:** 1111–1149.

FOWLER, S. W., AND G. A. KNAUER. 1986. Role of large particles
in the transport of elements and organic compounds through
the oceanic water column. Prog. Oceanogr. **16:** 147–194.

FUH, C. B., M. N. MYERS, AND J. C. GIDDINGS. 1992. Analytical
SPLITT fractionation: Rapid particle size analysis and mea-
surements of oversized particles. Anal. Chem. **64:** 3125–3132.

GARDNER, W. D. 1980. Sediment trap dynamics and calibration: A
laboratory evaluation. J. Mar. Res. **38:** 17–39.

———. 1997. The flux of particles to the deep sea: Methods, mea-
surements, and mechanisms. Oceanography **10:** 16–21.

GIBBS, R. J. 1981. Floc breakage by pumps. J. Sediment. Petrol.
51: 670–672.

GIDDINGS, J. C. 1985. A system based on split-flow lateral transport
thin (SPLITT) separation cells for rapid and continuous particle
fractionation. Specul. Sci. Technol. **20:** 749–768.

GOLDMAN, J. C. 1988. Spatial and temporal discontinuities of bio-
logical processes in pelagic surface waters, p. 273–296. *In* B.
Rotschield [ed.], Toward a theory on biological-physical inter-
actions in the World Ocean. Kluwer.

GUST, G., W. BOWLES, S. GIORDANO, AND M. HUTTEL. 1996. Par-
ticle accumulation in a cylindrical sediment trap under laminar
and turbulent steady flow: An experimental approach. Aquat.
Sci. **58:** 297–326.

———, R. H. BYRNE, R. E. BERNSTEIN, P. R. BETZER, AND W.
BOWLES. 1992. Particle flux and moving fluids: Experience
from synchronous trap collections in the Sargasso Sea. Deep-
Sea Res. **39:** 1071–1083.

———, AND H.-P. KOZERSKI. 2000. In situ sinking-particle fluxes
from collection rates of cylindrical traps. Mar. Ecol. Prog. Ser.
In press.

GUSTAFSSON Ö., K. O. BUESSELER, AND P. M. GSCHWEND. 1996.
On the integrity of cross-flow filtration for collecting marine
organic colloids. Mar. Chem. **55:** 93–111.

———, AND P. M. GSCHWEND. 1997. Aquatic colloids: Concepts,
definitions, and current challenges. Limnol. Oceanogr. **42:**
519–528.

———, F. HAGHSETA, C. CHAN, J. McFARLANE, AND P. M.
GSCHWEND. 1997. Quantification of the dilute sedimentary
soot-phase: Implications for PAH speciation and bioavailabil-
ity. Environ. Sci. Technol. **31:** 3544–3550.

———, A. WIDERLUND, P. S. ANDERSSON, J. INGRI, P. ROOS, AND
A. LEDIN. 2000. Colloid dynamics and transport of major el-
ements through a boreal river—brackish bay mixing zone. Mar.
Chem. **71:** 1–21.

HEISKANEN, A.-S., AND J.-M. LÄPPANEN. 1995. Estimation of export
production in the coastal Baltic Sea: Effect of resuspension and
microbial decomposition on sedimentation measurements. Hy-
drobiologica **316:** 211–224.

HOBRO, R. 1979. Annual phytoplankton successions in a coastal
area in the northern Baltic, p. 3–10 *In* E. Naylor and R. G.
Hartnoll [eds.], Cyclic phenomena in marine plants and ani-
mals. Pergamon.

INGRI, J., R. LÖFVENDAHL, AND K. BOSTRÖM. 1990. Chemistry of suspended particles in the southern Baltic Sea. Mar. Chem. **32:** 73–87.

———, AND A. WIDERLUND. 1994. Uptake of alkaline and alkaline-earth elements on suspended iron and manganese in the Kalix River, northern Sweden. Geochim. Cosmochim. Acta **58:** 5433–5442.

———, ———, M. LAND, Ö. GUSTAFSSON, P. ANDERSSON, AND B. ÖHLANDER. 2000. Temporal variations in the fractionation of the rare earth elements in a boreal river: The role of colloidal particles. Chem. Geol. **166:** 23–45.

KEIL, R. G., E. TSAMAKIS, C. B. FUH, J. C. GIDDINGS, AND J. I. HEDGES. 1994. Mineralogical and textural controls on the organic composition of coastal marine sediments: Hydrodynamic separation using SPLITT-fractionation. Geochim. Cosmochim. Acta **58:** 879–893.

KEPKAY, P. E., S. E. H. NIVEN, AND J. F. FELLET. 1997. Colloidal organic carbon and phytoplankton speciation during a coastal bloom. J. Plankton Res. **19:** 369–389.

KNAUER, G., D. M. KARL, J. H. MARTIN, AND C. N. HUNTER. 1984. In situ effects of selected preservatives on total carbon, nitrogen, and metals collected in sediment traps. J. Mar. Res. **42:** 445–462.

KRAUSKOPF, K. B., AND D. K. BIRD. 1995. Introduction to geochemistry, McGraw-Hill.

LEAD, J. R., W. DAVISON, J. HAMILTON-TAYLOR, AND J. BUFFLE. 1997. Characterizing colloidal material in natural waters. Aquat. Geochem. **3:** 213–232.

LEVIN, S., AND G. TAWIL. 1993. Analytical SPLITT fractionation in the diffusion mode operating as a dialysis-like system devoid of membrane. Application to drug-carrying liposomes. Anal. Chem. **65:** 2254–2261.

MICHAELS, A. F., M. W. SILVER, M. M. GOWING, AND G. A. KNAUER. 1990. Cryptic zooplankton swimmers in upper ocean sediment traps. Deep-Sea Res. **37:** 1285–1296.

MORAN, S. B., M. A. CHARETTE, S. M. PIKE, AND C. A. WICKLUND. 1999. Differences in seawater particulate organic carbon concentration in samples collected using small- and large-volume methods: The importance of DOC adsorption to the filter blank. Mar. Chem. **67:** 33–42.

PONTÉR, C., J. INGRI, J.-O. BURMAN, AND K. BOSTRÖM. 1990. Temporal variations in dissolved and suspended iron and manganese in the Kalix River, northern Sweden. Chem. Geol. **81:** 121–131.

SAMBROTTO, R. N., AND OTHERS. 1993. Elevated consumption of carbon relative to nitrogen in the surface ocean. Nature **363:** 248–250.

WAITE, A., P. K. BIENFANG, AND P. J. HARRISON. 1992. Spring bloom sedimentation in a subarctic ecosystem. II. Succession and sedimentation. Mar. Biol. **114:** 131–138.

WAKEHAM, S. W., J. I. HEDGES, C. LEE, AND T. K. PEASE. 1993. Effects of poisons and preservatives on the composition of organic matter in a sediment trap experiment. J. Mar. Res. **51:** 661–696.

WALVE, J., AND U. LARSSON. 1999. Carbon, nitrogen, and phosphorous stoichiometry of a crustacean zooplankton in the Baltic Sea: Implications for nutrient recycling. J. Plankton Res. **21:** 2309–2321.